Physics Letters A 379 (2015) 962–967

Contents lists available at ScienceDirect

Physics Letters A

www.elsevier.com/locate/pla

Non-linear instability of a thin film flowing down a cooled wavy thick wall of finite thermal conductivity

L.A. Dávalos-Orozco

Instituto de Investigaciones en Materiales, Departamento de Polímeros, Universidad Nacional Autónoma de México, Ciudad Universitaria, Circuito Exterior S/N, Delegación Coyoacán, 04510 México DF, Mexico

ARTICLE INFO

Article history:
Received 2 December 2014
Received in revised form 19 January 2015
Accepted 20 January 2015
Available online 22 January 2015
Communicated by C.R. Doering

Keywords:
Thin liquid film
Inclined plane
Deformed thick wall
Marangoni effect
Thermocapillarity
Cooled from the wall

ABSTRACT

The flow of a thin film down a vertical cold thick wall with finite thermal conductivity is investigated under the lubrication approximation. It is shown that, despite the cooling from the wall, it is possible to find a new flow instability. That is, the free surface response to the wall deformation increases its amplitude with the negative Marangoni number. This amplitude growth is independent from the evolution of the time-dependent perturbations imposed on the free surface which, in contrast, are stabilized by cooling from the wall. However it is demonstrated that, even in this case, spatial resonance (see Dávalos-Orozco, 2007, 2008) is more effective to stabilize the time-dependent perturbations. From the results it is evident that these effects are possible only when the magnitudes of the thicknesses ratio and the thermal conductivities ratio are small.

1. Introduction

In real world applications, like surface coating and cooling, the thin liquid films are laid on walls with finite thickness and thermal conductivities. Therefore the recent interest in the investigation of the stability of these films under flow. The motivation for taking different thermal and mechanical wall conditions varies according to the goal of the problem.

Oron et al. [1] investigate evaporative instabilities of thin films. They need to introduce the thickness of the wall to eliminate singularities at the rupture point. Kabova et al. [2] include the thickness of the wall in order to introduce a wall surface topography which is related to experimental settings. Gambaryan-Roisman [3] investigates the stability of a thin film on a wall with non-uniform thermal conductivity. The results are obtained proposing a relation between this non-uniformity and the thickness of the wall. Gambaryan-Roisman and Stephan [4] investigate the effect of longitudinal topography of a thick wall in the formation of rivulets. They include the Lennard-Jones potential in their calculations.

The above mentioned papers motivated a systematic numerical calculation on the nonlinear instability of a thin film flowing down a heated thick wall [5]. In that paper, it is found that the thermal instability is governed by the Marangoni number Ma, the Biot number at the interface of the liquid and the atmosphere (at the free surface) and by d and Q_C. Here, d is the thicknesses ratio of the wall over that of the liquid film and Q_C is the thermal conductivities ratio of the wall over that of the liquid film. These two parameters only appear forming the ratio d/Q_C under the lubrication approximation [6–8] (for a recent review see [9]). The ratio d/Q_C appears in the denominator of the thermocapillary term and consequently its growth has an important stabilizing effect.

The flow down a sinusoidal wall has been investigated under the lubrication approximation by Dávalos-Orozco [10,11]. It is shown that by means of spatial resonance it is possible to stabilize the time-dependent perturbation, even when the fluid is viscoelastic [12]. These particular wall deformations may work as a filter for the perturbations in a finite region of the wall [11] (see a review in [9]). At resonance the wavelength of the wall deformation approaches to that of the time-dependent perturbations and the amplitude of the free surface response increases lowering its valley. Therefore, near to the valley the film is very thin and hence has a local stabilizing effect from which the time-dependent perturbations are not able to recover [10]. The instability of a film flowing down a heated wavy wall was investigated by D'Alessio et al. [13]. Notice that nonlinear results of a Benney type equation under the lubrication approximation are presented in Dávalos-Orozco [9]. It is demonstrated that it is still possible to stabilize the time-dependent perturbations by means of spatial resonance when the wall is an ideal very good conductor.

This last problem has been extended to the case of a heated thick wavy wall with finite thermal conductivity [14]. A nonlinear

E-mail address: ldavalos@unam.mx.

http://dx.doi.org/10.1016/j.physleta.2015.01.018
0375-9601/

Nomenclature

A	air jet maximum time-dependent pressure	T_L	wall lower face temperature
a	air jet time-dependent pressure dispersion	T_{wall}	wall temperature
B	wall deformation amplitude	T_0	zeroth order fluid temperature
Bi	Biot number	u	velocity x-component
c	phase velocity	v	velocity y-component
d	d_{wall}/h_0	w	velocity z-component
d_{wall}	wall thickness	x	non-dimensional x coordinate
$h(x, y, t)$	film local thickness	y	non-dimensional y coordinate
$H(x, y, t)$	film local perturbation	z	non-dimensional z coordinate
h_0	unperturbed film thickness	z^*	dimensional z coordinate
H_h	heat transfer coefficient	*Greek*	
k	wavenumber		
k_f	fluid heat conductivity	β	wall inclination angle
k_{wall}	wall heat conductivity	Δ	means difference
L	wall wavelength over perturbations wavelength ratio	ε	wave slope smallness parameter
Ma	Marangoni number	ζ	wall deformation
P_p	surface external pressure	κ	thermal diffusivity
Pr	Prandtl number	λ	wavelength
$Q_c = k_{wall}/k_f$	wall over fluid conductivities ratio	ν	kinematic viscosity
R	Reynolds number	ρ	fluid density
S	scaled surface tension number	σ	surface tension
T	fluid temperature	Σ	surface tension number
$T_{ambient}$	ambient atmosphere temperature	ω	frequency of oscillation

evolution equation of the Benney type is calculated which includes in the denominator of the thermocapillary term an extra spatial variation due to the waviness of the wall. A bump in the free surface response is found near to the valley (the thinnest part) of the wall deformation producing a reduction in the amplitude.

In this paper it will be demonstrated that, when cooling from the wall and the Marangoni number is negative, it is possible to destabilize the thin film free surface response to the wall deformation. The paper is organized as follows. In the next section a brief presentation of the physics of the problem is given along with the evolution equation of the thin film obtained from the basic equations of motion and heat transfer. In Section 3, the numerical results of the evolution equation are exposed graphically and explained in detail. The last section are the conclusions.

2. Thermocapillary flow of a thin film down a cooled wavy thick wall

The system under investigation is a thin film flowing down a cooled wall which has finite thickness and thermal conductivity. The system is sketched in Fig. 1 in non-dimensional form. There, the coordinate system is defined in relation with a flat surface which represents the mean of the wavy deformed wall. Therefore, the x-direction corresponds to the direction of the main velocity of the film. This is perpendicular to the z-direction crossing the film thickness and pointing outwards the fluid film. Assuming a right-handed system, the y-direction is perpendicular to these two. It is assumed that the temperature of the lower face of the wall is T_L and it is located at $z^* = -d_{wall}$ (the star means dimensional), where d_{wall} is the thickness of the wall. The thickness of the film is h_0. It is assumed that the ambient atmosphere above the free surface has a temperature $T_{ambient} > T_L$.

A smallness parameter $\varepsilon = 2\pi h_0/\lambda \ll 1$ is used for the asymptotic expansion of the variables. λ is a representative long wavelength of the perturbations which means that the slope of the free surface deformation is small.

The variables are made non-dimensional by means of h_0 for distance in the z-direction, $\lambda/2\pi$ for distance in the x- and

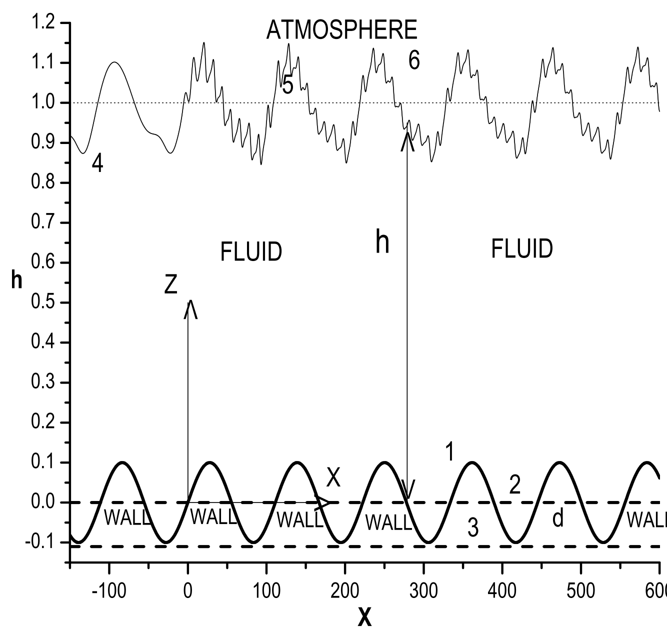

Fig. 1. The thin film and cooled wall assumed vertical. The mean non-dimensional wall thickness is $d = 0.11$. 1) Wall sinusoidal deformation (solid), 2) Mean height of the wall (dashed), 3) Lower side of the wall located at $z = -0.11$ (dashed) with non-dimensional temperature 1, lower than that of the atmosphere above the free surface. 4) Free surface response to the wall deformation, 5) Mean height of the unperturbed free surface (dotted), 6) Time-dependent perturbations excited at $x = 0$ and running on the free surface response. They have a local height $h(x, t)$ with respect to the wall deformation. The largest and smallest thickness of the wall are 0.21 and 0.01, respectively.

y-directions, $h_0\lambda/(\nu 2\pi)$ for time, ν/h_0 for velocity, $\rho\nu^2/h_0^2$ for pressure and $\Delta T = (T_L - T_{ambient}) < 0$ for temperature. The kinematic viscosity and the density are ν and ρ, respectively.

In non-dimensional form the free surface is assumed to be located at $z = \zeta(x, y) + 1$ before the application of a perturbation, where $\zeta(x, y)$ is the wall deformation. When the surface is perturbed the location is set as $z = \zeta(x, y) + h(x, y, t)$ where

$h(x,y,t) = 1 + H(x,y,t)$. As seen in Fig. 1, the wall lower face is now located at $z = -d = -d_{wall}/h_0$. The angle of inclination of the wall is assumed here to fixed at $\beta = 90°$.

Variables expansions are introduced (see [14]) in the scaled and non-dimensional Navier–Stokes, continuity and heat diffusion equations and their corresponding boundary conditions. The expansions are:

$$u = u_0 + \varepsilon u_1 + \cdots, \qquad v = v_0 + \varepsilon v_1 + \cdots,$$
$$w = \varepsilon(w_1 + \varepsilon w_2 + \cdots), \qquad p = p_0 + \varepsilon p_1 + \cdots,$$
$$T = T_0 + \varepsilon T_1 + \cdots, \qquad T_{wall} = T_{wall0} + \varepsilon T_{wall1} + \cdots. \tag{1}$$

The calculated main velocity and temperature profiles are :

$$u_0 = -\frac{1}{2} R \sin\beta \big(z - \zeta(x,y)\big)\big(z - \zeta(x,y) - 2h(x,y,t)\big) \tag{2}$$

$$T_{wall0} = \frac{Q_C(1 + Bi\,h(x,y,t)) - Bi(z - \zeta(x,y))}{Q_C(1 + Bi\,h(x,y,t)) + Bi(d + \zeta(x,y))} \tag{3}$$

$$T_0 = \frac{Q_C(1 + Bi\,h(x,y,t)) - Bi\,Q_C(z - \zeta(x,y))}{Q_C(1 + Bi\,h(x,y,t)) + Bi(d + \zeta(x,y))} \tag{4}$$

Notice that at the wall, $z = \zeta(x,y)$, the main velocity $u_0 = 0$, the temperature $T_0 = T_{wall0}$ and the heat flux boundary condition is satisfied. At the free surface $du_0/dz|_{z=\zeta(x,y)+h(x,y,t)} = 0$. Besides, $T_{wall0} = 1$ at $z = -d$. Observe that T_{wall0} and T_0 have the same formulas as in the case of heating from below [14]. The reason is that when cooling from below the temperature is made non-dimensional by means of the same term ΔT, which now is negative. This corrects the sign of both temperature profiles.

At the first order of the expansion the free surface kinematic boundary condition gives:

$$\begin{aligned} &h_t + \mathrm{R}\sin\beta h^2 h_x + \varepsilon \Bigg\{ (\mathrm{R}\sin\beta)^2 \left(\frac{2}{15} h^6 h_x\right)_x \\ &+ \frac{1}{3}\nabla\cdot\Bigg[h^3\big(-\mathrm{R}\cos\beta\nabla(\zeta + h) + 3\mathrm{S}\nabla^2\nabla(\zeta + h) - \nabla P_p\big) \\ &+ \frac{3}{2}\frac{Ma}{Pr}\frac{Bi\,h^2[\nabla h + \frac{1}{Q_C}\nabla\zeta]}{(1 + Bi[h + \frac{1}{Q_C}\zeta + \frac{d}{Q_C}])^2}\Bigg]\Bigg\} = 0, \end{aligned} \tag{5}$$

which is a Benney type evolution equation for the free surface deformation. Here, $\nabla = (\partial/\partial x, \partial/\partial y)$ is the horizontal nabla operator. The Prandtl number is $Pr = \nu/\kappa$ (where κ is the fluid thermal diffusivity), the Reynolds number is $R = gh_0^3/\nu^2$, the Marangoni number is $Ma = (-d\sigma/dT)\Delta T h_0/(\rho\nu\kappa)$ and the Biot number is $Bi = H_h h_0/k_f$. H_h is the coefficient of heat transfer, K_f is the heat conductivity of the fluid, $S = \varepsilon^2\Sigma$ and $\Sigma = \sigma h_0/3\rho\nu^2$ with σ the surface tension. Notice that when $\zeta(x,y) = 0$ this equation reduces to that obtained by Dávalos-Orozco [5]. However, when $Q_C \to \infty$ (very good conducting wall) the wall deformation effect disappears from the thermocapillary term and the equation reduces to Eq. A3 in the appendix of D'Alessio et al. [13]. When $Ma = 0$ it reduces to that of Dávalos-Orozco [10,11]. If the wall is flat $\zeta = 0$ and $Ma = 0$, the equation reduces to a perturbed Benney equation [8]. In case $P_p = 0$ the equation reduces to that of Benney [15,6,7]. It is important to point out that the effect of cooling from the wall is only reflected in the negative Marangoni number.

The function

$$P_p(x,y,t) = A\left|\sin\frac{\omega}{2}t\right|\exp\big[-a\big(x^2 + y^2\big)\big] \tag{6}$$

is assumed to represent a free surface time-dependent pressure due to a turbulent air jet striking periodically on the free surface around the origin (see [16]). The parameters will be fixed as $A = 0.0001$ and $a = 0.05$ in order to avoid non-saturating very large amplitude time-dependent perturbations. Here, ω is the frequency of oscillation of the time-dependent perturbations, which is divided by two because a jet has no suction (therefore the absolute value of the sine function). It will be effective only when it strikes again (with positive sign) on the surface. The wall deformation with an amplitude B is defined as $\zeta(x) = B\sin[xk/L]$ where $k = \omega/R\sin\beta$ is the wavenumber corresponding to a given ω, R and β of the time-dependent perturbations. In fact this last relation comes from the phase velocity of the linearized version of Eq. (5) which is represented by $c = R\sin\beta = \omega/k$. The parameter L is a real number representing the ratio of the wall wavelength over the wavelength of the time-dependent perturbations. This means that the wall wavelength is measured in terms of the wavelength of the time-dependent perturbations.The following section presents the numerical analysis of Eq. (5).

3. Numerical analysis of the Benney type equation

Here the numerical results of the Benney type Eq. (5) are presented. Finite differences are used in space and time to follow the evolution of the time-dependent perturbations and the free surface response to the wall deformations.

The number of parameters is large and some of them will be fixed in the present problem. The fixed parameters are $A = 0.0001$, $a = 0.05$, $B = 0.1$, $d = 0.11$, $Pr = 7$, $S = 1$, $\varepsilon = 0.1$ and $\beta = 90°$ for a vertical wall. The other parameters Bi, L, Ma, Q_C, R and ω are varied in a convenient way in order to show the main results of the paper. The number of parameters is still large. Therefore, the ω and R (and the corresponding wavelength) are selected as those corresponding to the maximum growth rate of the isothermal problem. The numerical calculations are done in a spatial range which is measured as $-150 \le x \le G\sin\beta \times \text{time} + 100$. Assuming that $h(x,t) = 1 + H(x,t)$, the boundary conditions are $H = dH/dx = 0$ at $x = -150$ and at $G\sin\beta \times \text{time} + 100$. "Time" means the running time shown in the figure captions. These conditions mean that the free surface is deformed like the wall does before it is let to respond in space and time to the wall deformation. Notice that in the figures only a range of the numerical calculations is given for the sake of presentation.

The initial results are for a Biot number $Bi = 0.1$. The first case corresponds to a small frequency of oscillation of the perturbation, that is, $\omega = 0.5$ and $R = 1.391$. The solutions are presented in Fig. 2 for two different circumstances. The first one for $L = 8$ is shown in Fig. 2a and the second one in Fig. 2b corresponds to spatial resonance already attained when $L = 5$. In this paper it is assumed that the wall is cooled from below. Thus, in Fig. 2a the perturbations decrease in space and time. Nevertheless, it is clear that resonance (when $L = 5$) is more effective to stabilize the time-dependent perturbations. Notice that for the sake of presentation and clarity, all the figures only present the spatial range $-150 \le x \le 600$. In all the figures the curve number 1 always corresponds to the wall wavy profile. The mean value of the other curves should be located one unit above the mean of curve 1 (at $h = 0$) but, for the sake of presentation, they are not plotted at their corresponding height. It is interesting to see that the amplitude of the free surface response to the wall deformation increases with the growth of the negative Marangoni number. The free surface response without time-dependent perturbations can clearly be seen in the range $-150 \le x \le 0$. The magnitude of the negative Ma increases from curve 2 to 4 when $Q_C = 0.01$ and from curve 5 to 7 when $Q_C = 0.05$. From the figures it is evident that the instability of the free surface response changes with Q_C. Notice that the magnitudes selected for Q_C are very small. These conditions are satisfied by a wall of new very insulating materials known as silica aerogels (see [21]) which have a typical heat conductivity of $k_{wall} = 0.015$ W/m K at ambient temperature, pressure

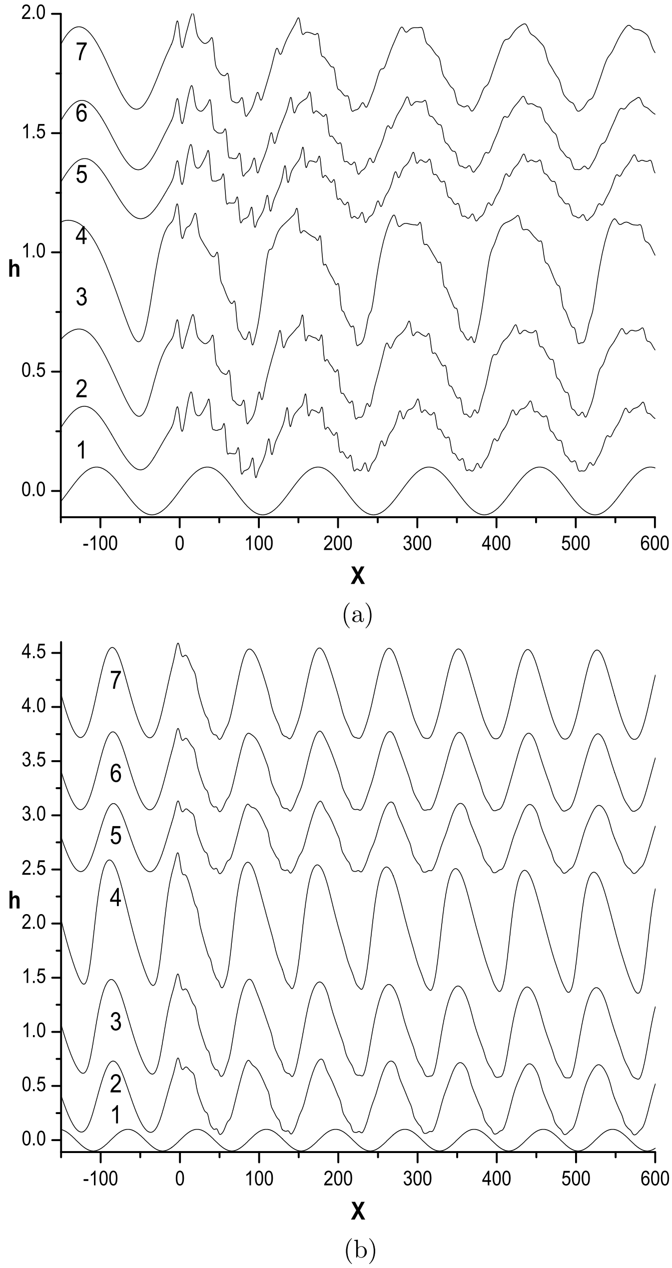

Fig. 2. Time = 1000, $Pr = 7$, $S = 1$, $Bi = 0.1$. $\omega = 0.5$, $R = 1.391$. 1) Wall. $Q_C = 0.01$: 2) $Ma = -10$, 3) $Ma = -50$, 4) $Ma = -100$. $Q_C = 0.05$: 5) $Ma = -10$, 6) $Ma = -50$, 7) $Ma = -100$. (a) $L = 8$ and (b) $L = 5$ (resonance). Notice pure responses from $x = -150$ to 0.

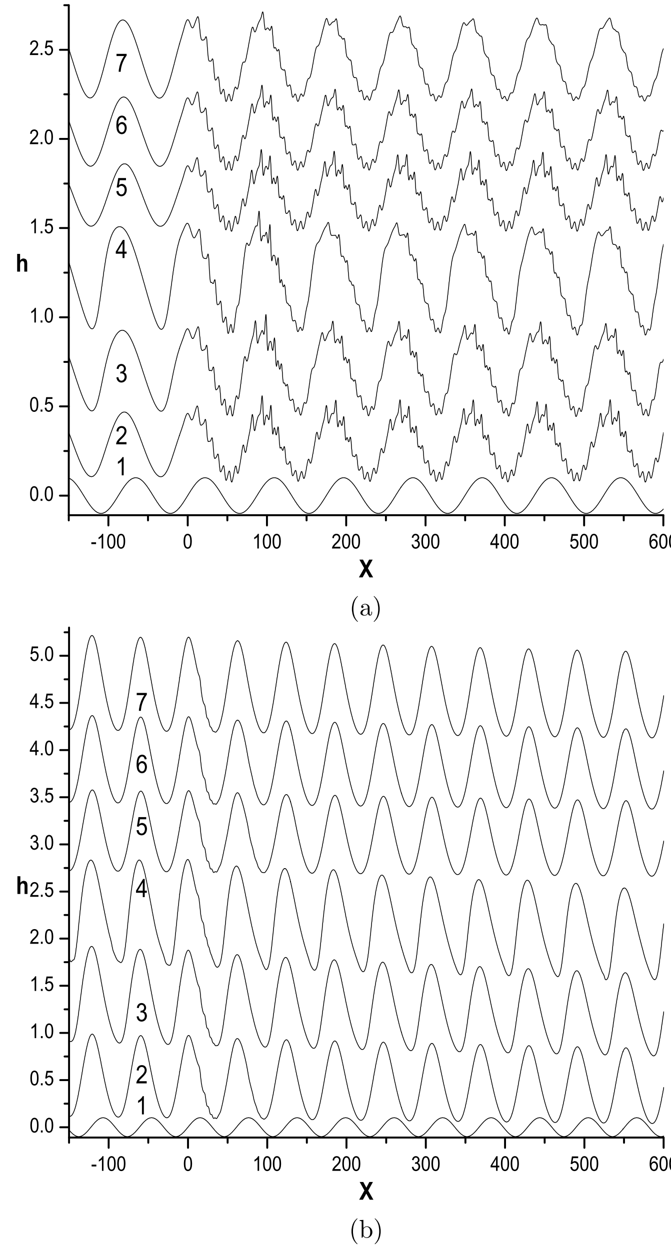

Fig. 3. Time = 600. $Pr = 7$, $S = 1$, $Bi = 0.1$. $\omega = 2$, $R = 2.783$. 1) Wall. $Q_C = 0.01$: 2) $Ma = -10$, 3) $Ma = -50$, 4) $Ma = -100$. $Q_C = 0.05$: 5) $Ma = -10$, 6) $Ma = -50$, 7) $Ma = -100$. (a) $L = 10$ and (b) $L = 7$ (resonance). Notice pure responses from $x = -150$ to 0.

and humidity. Moreover, they can be produced into very thin solid films.

The results of Fig. 3 are for a different frequency $\omega = 2$ and a higher Reynolds number 2.783. The parameters are responsible for an amplitude increase of the free surface response. In Fig. 3a the time-dependent perturbations imposed at $x = 0$ decrease in space due to the cooling of the wall. Nevertheless, according to the magnitude of $Ma < 0$ the perturbations are more or less stabilized. The amplitude increase of the free surface response with respect to that of Fig. 2 can be understood by the new vertical scaling used in Fig. 3. Observe that when $L = 7$ resonance is more effective than cooling to stabilized the perturbations in a shorter spatial range. Both cooling and resonance effects work together to further destabilize the free surface response.

Two more examples are presented for a different Biot number, $Bi = 1$. For $\omega = 0.5$ and $R = 1.391$, Fig. 4 shows that the curves of the free surfaces response have an instability not found before. That is, they present a distortion near to the valleys of the wall. This distortion occurs simultaneously to an amplitude increase of the response when $Ma < 0$ increases. In general, the lowest region of the response moves to the right and closer to the thinnest part of the wall, where the cooling is more effective. The distortion is more important at spatial resonance ($L = 5$) and for a larger magnitude of $Ma < 0$.

The values $\omega = 2$ and $R = 2.783$ lead to the interesting result that, despite being outside resonance for $L = 8$, the flow stabilizes more effectively with the negative Marangoni number, as seen in Fig. 5a. This is due to the important influence of the higher Biot number used here, which allows for more heat flux through the free surface. It is significant that the free surface response destabi-

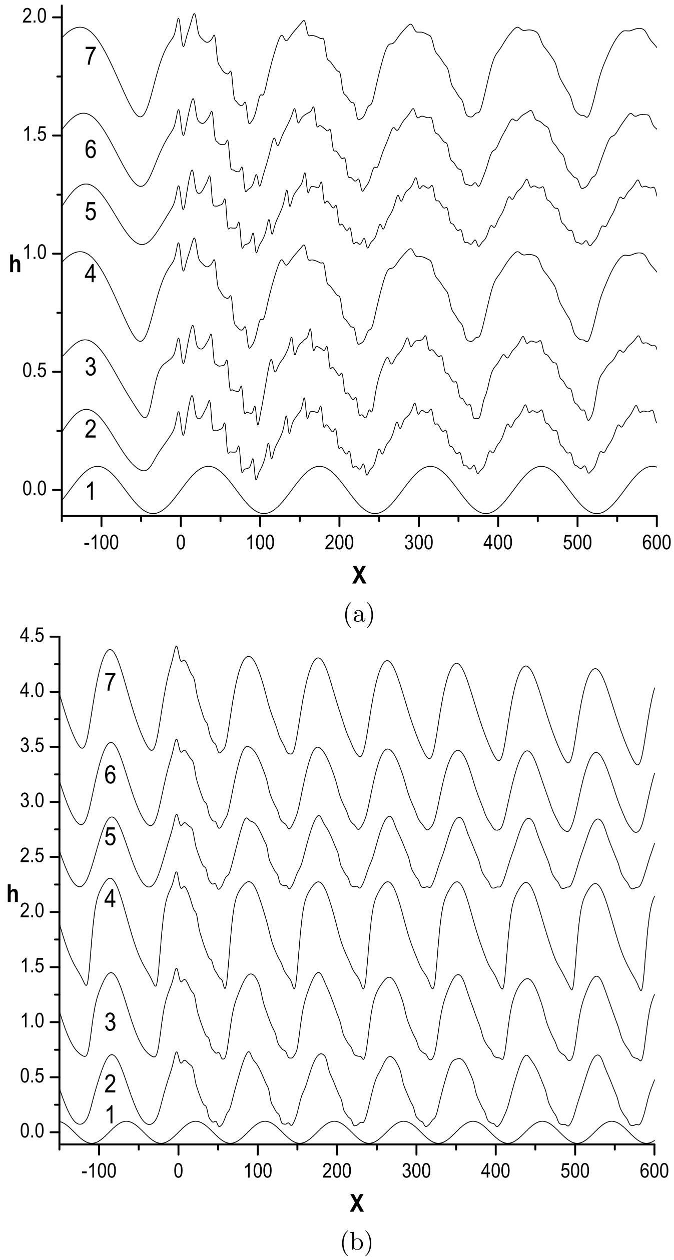

Fig. 4. Time $= 1000$, $Pr = 7$, $S = 1$, $Bi = 1$. $\omega = 0.5$, $R = 1.391$. 1) Wall. $Q_C = 0.01$: 2) $Ma = -10$, 3) $Ma = -50$, 4) $Ma = -100$. $Q_C = 0.05$: 5) $Ma = -10$, 6) $Ma = -50$, 7) $Ma = -100$. (a) $L = 8$ and (b) $L = 5$ (resonance). Notice pure responses from $x = -150$ to 0.

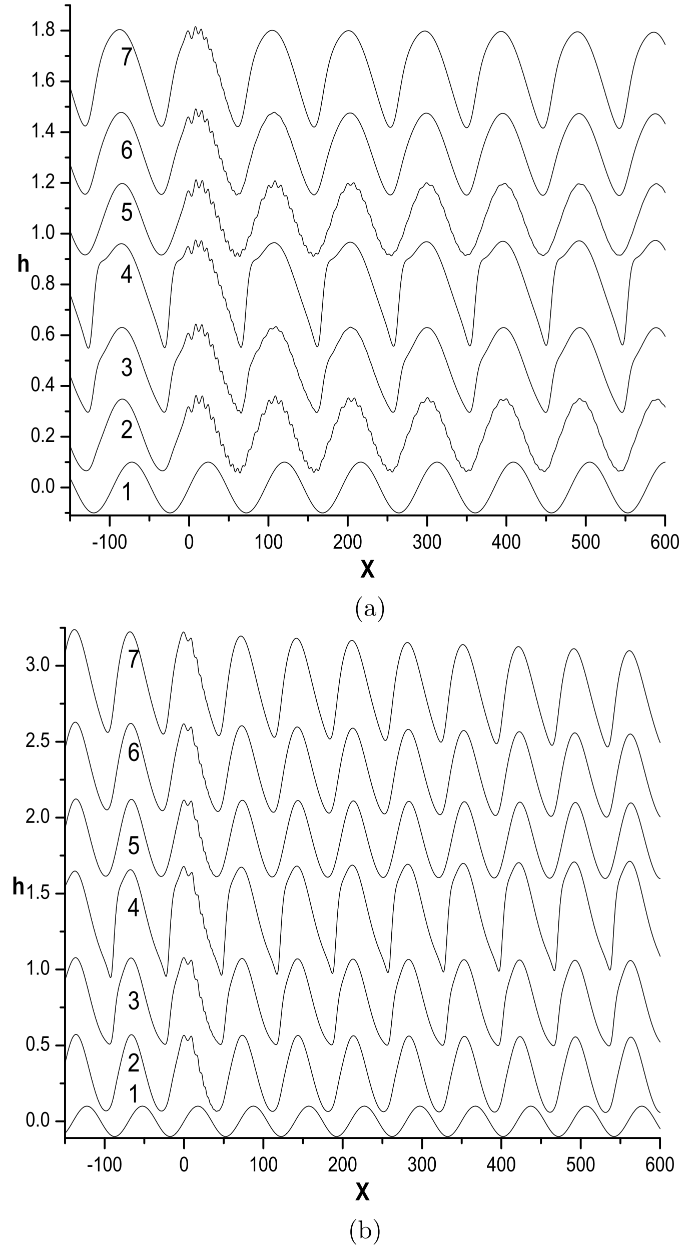

Fig. 5. Time $= 600$, $Pr = 7$, $S = 1$, $Bi = 1$. $\omega = 2$, $R = 2.783$. 1) Wall. $Q_C = 0.01$: 2) $Ma = -10$, 3) $Ma = -50$, 4) $Ma = -100$. $Q_C = 0.05$: 5) $Ma = -10$, 6) $Ma = -50$, 7) $Ma = -100$. (a) $L = 11$ and (b) $L = 8$ (resonance). Notice pure responses from $x = -150$ to 0.

lizes still more with the negative Marangoni number. Besides, the distortion around the valley is even more pronounced and now it moves to the right, closer to the thinnest part of the wall, where heat conductivity improves. This effect is stronger when resonance takes place in Fig. 5b for $L = 8$.

4. Conclusions

The free surface response to the wall deformation is found to destabilize with the negative Marangoni number for different magnitudes of Q_C and a small magnitude of d (here fixed as 0.11). From the analytical point of view, this is due to the spatial derivatives of the numerator and denominator of the nonlinear thermocapillary term, the last one in Eq. (5). In particular, the x-derivative takes factors from the denominator into the numerator which have important influence when the parameter Q_C is small. Furthermore, owing to the stabilizing effects of d found recently [5,14], it is necessary to select $d \ll 1$.

The physical explanation of this phenomenon is the sudden strong cooling felt by the free surface when it approaches to the thinnest region of the wall. There the surface tension is stronger than that at the top of the free surface response. This produces a shear flow from the top to the valley which enhances the depression of the response. The shear flow, and therefore the growth in amplitude, is more important increasing the negative magnitude of Ma.

In the case of a sudden heating, as when the film flows down a locally heated plate (see [17–20] and [9] for a review), a high bump of the free surface response appears above the upper side of the plate. On the contrary, if the same experiment were done for flow on a cold plate, there should appear a low depression of the thin film. That bump was found in the previous paper [14]. The results were different, yet unexpected. In contrast, here a huge depression is found due to the sudden cooling near the thinnest section of the wall. It is interesting that this amplitude growth is reinforced by the spatial resonance effect where the amplitude of the free surface response has a further increase. The results also made it clear that spatial resonance is more effective to stabilize in space and time the time-dependent perturbations than the cooling from the wall.

In this paper the joint effects on a thin film of wall thickness, finite thermal conductivity, topography and cooling from the wall were investigated. It is concluded that, as demonstrated above, they are able to produce the cooling instability of the free surface response for a range of magnitudes of Q_C and d around those investigated here.

Acknowledgements

The author would like to thank Joaquín Morales, Cain González, Alberto López, Raúl Reyes, Ma. Teresa Vázquez and Oralia Jiménez for technical support.

References

[1] A. Oron, S.G. Bankoff, S.H. Davis, Phys. Fluids 8 (1996) 3433.
[2] Yu.O. Kabova, A. Alexeev, T. Gambaryan-Roisman, P. Stephan, Phys. Fluids 18 (2006) 012104.
[3] T. Gambaryan-Roisman, Int. J. Heat Mass Transf. 53 (2010) 390.
[4] T. Gambaryan-Roisman, P. Stephan, J. Heat Transf. 131 (2009) 033101.
[5] L.A. Dávalos-Orozco, Int. J. Non-Linear Mech. 47 (2012) 1.
[6] S.W. Joo, S.H. Davis, S.G. Bankoff, J. Fluid Mech. 230 (1991) 117.
[7] S.W. Joo, S.H. Davis, J. Fluid Mech. 242 (1992) 529.
[8] L.A. Dávalos-Orozco, S.H. Davis, S.G. Bankoff, Phys. Rev. E 55 (1997) 374.
[9] L.A. Dávalos-Orozco, Interf. Phenom. Heat Transf. 1 (2013) 93.
[10] L.A. Dávalos-Orozco, Phys. Fluids 19 (2007) 074103.
[11] L.A. Dávalos-Orozco, Microgravity Sci. Technol. 20 (2008) 225.
[12] L.A. Dávalos-Orozco, Interf. Phenom. Heat Transfer 4 (2013) 301.
[13] S.J.D. D'Alessio, J.P. Pascal, H.A. Jasmine, K.A. Ogden, J. Fluid Mech. 665 (2010) 418.
[14] L.A. Dávalos-Orozco, Interf. Phenom. Heat Transfer 2 (2014) 55.
[15] D.J. Benney, J. Math. Phys. 45 (1966) 150.
[16] D. Lacanette, A. Gosset, S. Vincent, J.M. Buchlin, E. Arquis, Phys. Fluids 18 (2006) 042103.
[17] A.M. Frank, O.A. Kabov, Phys. Fluids 18 (2006) 032107.
[18] N. Tiwari, Z. Mester, J.M. Davis, Phys. Rev. E 76 (2007) 056306.
[19] E.A. Chinnov, E.N. Shatskii, Tech. Phys. Lett. 36 (2010) 53–56.
[20] Yu. Kabova, V.V. Kuznetsov, O. Kabov, T. Gambaryan-Roisman, P. Stephan, Int. J. Heat Mass Transf. 68 (2014) 527–541.
[21] A.C. Pierre, A. Rigacci, SiO_2 aerogels, in: M.A. Aegerter, N. Leventis, M.M. Koebel (Eds.), Aerogels Handbook, Springer, New York, 2011, Chapter 2.